Acta Crystallographica Section D
Biological Crystallography
ISSN 0907-4449

Crystallization of $[Fe_3S_4]$-ferredoxin from the hyperthermophile archaeon *Pyrococcus furiosus*

Michael S. Nielsen, Pernille Harris* and Hans E. M. Christensen

Department of Chemistry, Building 207, Technical University of Denmark, 2800 Kgs. Lyngby, Denmark

Correspondence e-mail: ph@kemi.dtu.dk

Received 28 August 2003
Accepted 25 September 2003

Recombinant *Pyrococcus furiosus* ferredoxin with a $[Fe_3S_4]$-cluster was crystallized through steps of optimization and X-ray diffraction data were collected from several crystal forms. Flat plate-like crystals were grown by hanging-drop vapour diffusion. The precipitant used was 30% PEG 400; the pH was varied between 7.0 and 8.0 and hexaamminecobalt(III) chloride was essential for crystal formation. The best crystals belong to space group $P2_1$, with unit-cell parameters a = 31.23, b = 47.51, c = 52.03 Å, β = 103.86°, and diffract to 1.5 Å resolution.

1. Introduction

Pyrococcus furiosus (DSM No. 3638) is a hyperthermophile archaeon with a growth optimum of 373 K originally isolated from a submarine volcanic area. The ferredoxin from *P. furiosus*, first described by Aono *et al.* (1989), is a small 66-amino-acid (7.5 kDa) electron-transfer protein which contains one $[Fe_4S_4]$-cluster (Fukuyama, 2001). It contains an unusual disulfide bond which is redox-active at approximately the same potential as the $[Fe_4S_4]$-cluster and exists in equilibrium between the *S* and *R* conformation (Wang *et al.*, 1999). Furthermore, an aspartate residue coordinates one of the Fe atoms in the iron–sulfur cluster and the $[Fe_4S_4]$-cluster readily converts to a $[Fe_3S_4]$-cluster under oxidizing conditions (Conover *et al.*, 1990). The ferredoxin is negatively charged at neutral pH, as is the case for other comparable ferredoxins (Fukuyama, 2001). A recent study suggested that *P. furiosus* ferredoxin is a dimer at physiological ionic strength, equivalent to 0.35 *M* NaCl (Hasan *et al.*, 2002).

The three-dimensional structure of *P. furiosus* ferredoxin is needed to obtain a better understanding of the hyperthermostable ferredoxins. This has so far been hampered by difficulties in obtaining crystals of satisfactory quality (Wang *et al.*, 1999). The *P. furiosus* ferredoxin has been crystallized as a complex with formaldehyde ferredoxin oxidoreductase (Hu *et al.*, 1999), but the electron-density map showed a disordered ferredoxin structure except at the interface region between the two proteins. The three-dimensional structure has also been investigated by NMR, but only a preliminary molecular model has been reported for the $[Fe_4S_4]$-ferredoxin (Sham *et al.*, 2002).

In this paper, we present the crystallization and preliminary X-ray characterization of the *P. furiosus* $[Fe_3S_4]$-ferredoxin.

2. Purification and crystallization

The gene encoding the *P. furiosus* ferredoxin was expressed in *Escherichia coli* and purified according to Zhang *et al.* (2003). The purified protein was lyophilized and stored at 253 K until crystallization experiments were carried out. Using mass spectrometry, the ferredoxin was verified to be the oxidized $[Fe_3S_4]$-ferredoxin with an intact disulfide bridge (Zhang *et al.*, 2003).

The lyophilized $[Fe_3S_4]$-ferredoxin was dissolved in 20 m*M* Tris–HCl pH 8.0 and filtered through a 0.22 µm filter (Millipore). The concentration of the protein was determined using UV–Vis spectroscopy and $\varepsilon_{380} = 17\,000\ M^{-1}\ cm^{-1}$ (Conover *et al.*, 1990).

Crystallization screens were performed using the sparse-matrix method (Jancarik & Kim, 1991) and crystalline precipitate was formed at pH values above 5.5 using polyethylene glycol as precipitant. An incomplete factorial design experiment was set up around these conditions (Carter & Carter, 1979). These experiments did not give any crystals but gave different types of aggregates.

The most promising precipitate was obtained with 30% PEG 4000, 0.1 *M* MES–NaOH pH 6.5, 0.15 *M* $CaCl_2$ and a protein solution with a concentration of 6.5 mg ml^{-1}. This condition, omitting the $CaCl_2$, was used with additives such as divalent cations, linkers and polyamines (Cudney *et al.*, 1994). The drops were set up with 2 µl reservoir solution, 2 µl protein solution and 0.25 µl of additive added to the drop. A snowflake-like crystal appeared (Fig. 1*a*) when hexaamminecobalt(III) chloride was used as an additive. The drop solution was clear close to the crystal arms, but coloured protein was seen in the solution further away from the crystal. Decreasing the solution viscosity should allow the protein to diffuse faster and exchange of PEG 4000 for PEG 400 did indeed change the

crystal growth to give small plate-like crystals. Further optimization was undertaken and the best crystals (Fig. 1*b*) were obtained using a reservoir solution consisting of 30%(*w*/*v*) PEG 400, 0.1 *M* HEPES–NaOH pH 7.4 or 0.1 *M* Tris–HCl pH 8.0 and a 2 µl drop of reservoir solution mixed with 2 µl of 6.5 mg ml^{-1} protein solution and 0.35 µl 0.1 *M* $[Co(NH_3)_6]Cl_3$. The drops were equilibrated against 500 µl reservoir solution at 277 K. The crystal plates grew within 2 d and often from a common nucleation point, but single crystal plates could easily be separated.

Electrochemical experiments with the ferredoxin have shown that neomycin is necessary for electron transfer (Zhang *et al.*, 2003). Moreover, it is evident from mass spectrometry that neomycin binds to ferredoxin in a 1:1 ratio at low ionic strength. Therefore, a protein solution was prepared containing an equimolar concentration of neomycin and crystallization trials were performed parallel to the initial screens as described above, giving similar results. When the importance of the addition of $[Co(NH_3)_6]Cl_3$ was realised, drops were set up in which neomycin and $[Co(NH_3)_6]Cl_3$ were added. The crystal plates that appeared when neomycin was added to the drop tended to be thinner than those without neomycin, but were still of diffraction quality.

Table 1
Data-collection and processing statistics for the ferredoxin crystals.

Values in parentheses are for the highest resolution shells.

	Ferredoxin with neomycin	Ferredoxin with neomycin	Ferredoxin without neomycin
Crystallization conditions			
Reservoir	31% PEG 400, 0.2 *M* HEPES–NaOH pH 7.0	29% PEG 400, 0.2 *M* HEPES–NaOH pH 7.0	30% PEG 400, 0.2 *M* Tris–HCl pH 8.0
Protein solution	6.5 mg ml^{-1} protein, 20 m*M* Tris–HCl pH 8.0, 0.87 m*M* neomycin	6.5 mg ml^{-1} protein, 20 m*M* Tris–HCl pH 8.0, 0.87 m*M* neomycin	6.5 mg ml^{-1} protein, 20 m*M* Tris–HCl pH 8.0
Additive to drop	0.1 *M* $[Co(NH_3)_6]Cl_3$	0.1 *M* $[Co(NH_3)_6]Cl_3$	0.1 *M* $[Co(NH_3)_6]Cl_3$
Drop size (µl)	2 + 2 + 0.35	2 + 2 + 0.30	2 + 2 + 0.30
Temperature (K)	277	277	277
Crystal dimensions (mm)	0.1 × 0.1 × 0.01	0.3 × 0.3 × 0.01	0.2 × 0.2 × 0.05
X-ray source	ID29, ESRF	ID14-4, ESRF	ID14-4, ESRF
Detector	ADSC Quantum CCD	ADSC Quantum CCD	ADSC Quantum CCD
Wavelength (Å)	0.9999	0.9393	0.9393
Data-collection temperature (K)	100	100	100
Resolution limit (Å)	35.00–2.25 (2.37–2.25)	34.71–1.75 (1.84–1.75)	34.6–1.5 (1.58–1.5)
No. reflections	21635	28550	76346
No. unique reflections	6314	13743	21276
Redundancy	3.4	2.1	3.6
Completeness (%)	94.8 (81.5)	85.9 (89.2)	89.8 (88.4)
R_{merge}†	0.10 (0.22)	0.13 (0.25)	0.10 (0.31)
$\langle I/\sigma(I)\rangle$	4.8 (2.7)	3.7 (2.4)	4.9 (2.2)
Space group	$P2_12_12_1$	$P2_1$	$P2_1$
Unit-cell parameters			
a (Å)	47.33	33.09	31.23
b (Å)	51.70	51.98	47.516
c (Å)	54.59	47.70	52.03
β (°)		101.09	103.86
Unit-cell volume (Å^3)	1.33 × 10^5	8.03 × 10^4	7.50 × 10^4
Solvent content (%)	45.1	54.4	51.1
V_M (Å^3 Da^{-1})	2.24	2.70	2.52
Mosaicity (°)	0.6–1.2	0.5–1.4	1.0–1.7
Wilson *B* factor (Å^2)	28.06	9.82	10.01

† $R_{merge} = \sum_i |I_i - \langle I_i\rangle| / \sum_i I_i$, where $\langle I_i\rangle$ is the average of I_i over all symmetry equivalents.

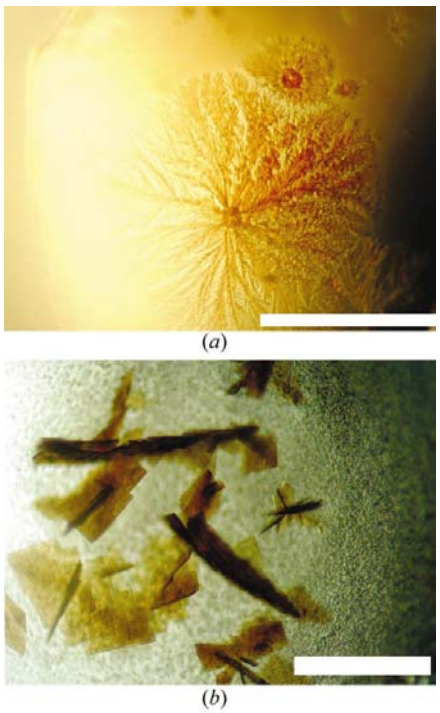

Figure 1
Crystals of *P. furiosus* ferredoxin. (*a*) Crystals formed using PEG 4000 as a precipitant. The white bar corresponds to 1 mm. (*b*) Crystals formed using PEG 400 as a precipitant. The white bar corresponds to 200 µm.

3. Preliminary X-ray characterization

Several crystals were tested at beamlines X11 and X13 at the EMBL Outstation in Hamburg. All crystals turned out to suffer from a large inhomogeneous mosaicity, giving rise to a powder-like streaky diffraction pattern when the incident X-ray beam was at the edge of the plate-shaped crystals, and we had problems indexing the diffraction patterns.

Diffraction data to 2.25 Å were collected on beamline ID-29, ESRF from a small crystal that was crystallized with neomycin in the drop. Although the diffraction pattern from this crystal is also streaky, it can be indexed in the orthorhombic crystal system. Freshly made crystals using slightly different crystallization conditions (Table 1) were brought to beamline ID14-4, ESRF and it was possible to collect data to 1.5 Å on a crystal grown without neomycin. The diffraction pattern from this crystal is shown in Fig. 2 for two crystal orientations rotated 90° with respect to each other. These data can be indexed using a monoclinic cell. Data to 1.8 Å were collected from a crystal grown with neomycin in the drop. These data could also be indexed in a monoclinic cell with somewhat different unit-cell parameters: the lengths of the *b* and *c* axes appear to have interchanged.

The intensities were integrated with *MOSFLM* (Leslie, 1992) and scaled with *SCALA* (Evans, 1993) from the *CCP*4 suite (Collaborative Computational Project, Number 4, 1994). The structure-factor amplitudes for all data sets were produced with *TRUNCATE* (French & Wilson, 1978). We decided to remove the worst-looking data (*i.e.* the data shown in Fig. 2*b*) where it is difficult to estimate intensities. This reduced the completeness to about 0.90, but improved the overall quality of the data considerably.

All three crystal forms are in accordance with two ferredoxin molecules in the asymmetric unit. For the orthorhombic crystal form, we have performed molecular replacement with the program *MOLREP* (Vagin & Teplyakov, 1997) using the peptide chain from *Thermotoga maritima* ferredoxin (PDB code 1vjw; Macedo-Ribeiro *et al.*, 1996) as the search model. We found a solution with two molecules in the asym-

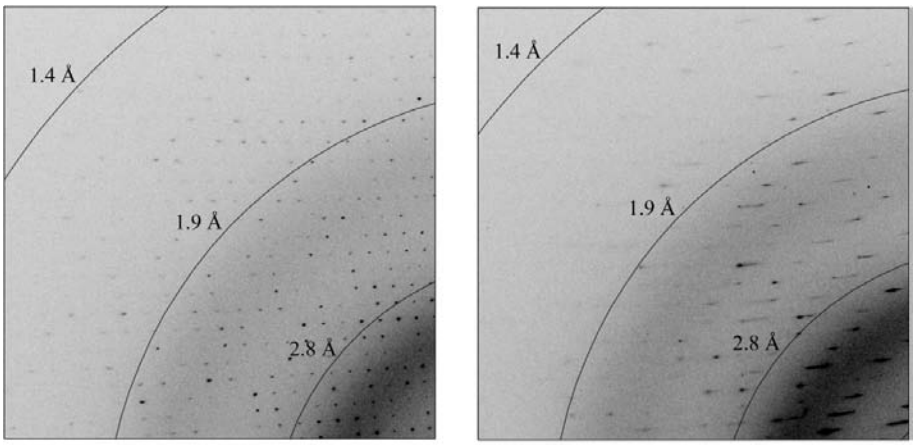

Figure 2
Diffraction images of *P. furiosus* ferredoxin crystals grown without neomycin collected at beamline ID14-4 at ESRF, Grenoble. (*a*) Rotation angle 0°, (*b*) rotation angle 90°.

metric unit, giving a correlation factor of 0.457 and an *R* factor of 0.623. A preliminary inspection of the map shows the $[Fe_3S_4]$-cluster in the correct position in both molecules. Furthermore, the map is traceable and the peptide chains can be extended to the correct length in both the N-terminal and the C-terminal directions. The structure determination is in progress and combination of the information from all three crystal forms will hopefully answer some of the questions related to dimerization and perhaps also to the role of neomycin.

Jens-Christian N. Poulsen, Heidi A. Ernst, Eva Johansson and Flemming Hansen from the University of Copenhagen are acknowledged for help with the crystallization and data collection. The EMBL Outstation in Hamburg is acknowledged for allocating beam time for the project. We acknowledge the European Synchrotron Radiation Facility for provision of synchrotron-radiation facilities and we would like to thank Andrew McCarthy for assistance in using beamline ID29 and Didier Nurizzo for assistance in using beamline ID14-4. Financial support to HEMC from the Danish Technical Science Research Council and to MSN from the Novo Scholarship Programme is acknowledged.

References

Aono, S., Bryant, F. O. & Adams, M. W. W. (1989). *J. Bacteriol.* **171**, 3433–3439.
Carter, C. W. Jr & Carter, C. W. (1979). *J. Biol. Chem.* **254**, 12219–12223.
Collaborative Computational Project, Number 4 (1994). *Acta Cryst.* D**50**, 760–763.
Conover, R. C., Kowal, A. T., Fu, W., Park, J.-B., Aono, S., Adams, M. W. W. & Johnson, M. K. (1990). *J. Biol. Chem.* **265**, 8533–8541.
Cudney, B., Patel, S., Weisgraber, K., Newhouse, Y. & McPherson, A. (1994). *Acta Cryst.* D**50**, 414–423.
Evans, P. R. (1993). *Proceedings of the CCP4 Study Weekend. Data Collection and Processing*, edited by L. Sawyer, N. Isaacs & S. Bailey, pp. 114–122. Warrington: Daresbury Laboratory.
French, G. S. & Wilson, K. S. (1978). *Acta Cryst.* A**34**, 517–525.
Fukuyama, K. (2001). *Handbook of Metalloproteins*, edited by A. Messerschmidt, R. Huber, T. Poulos & K. Wieghardt, pp. 543–552. Chichester: John Wiley & Sons.
Hasan, M. N., Hagedoorn, P. L. & Hagen, W. R. (2002). *FEBS Lett.* **531**, 335–338.
Hu, Y., Faham, S., Roy, R., Adams, M. W. W. & Rees, D. C. (1999). *J. Mol. Biol.* **286**, 899–914.
Jancarik, J. & Kim, S.-H. (1991). *J. Appl. Cryst.* **24**, 409–411.
Leslie, A. G. W. (1992). *Jnt CCP4/ESF–EACMB Newsl Protein Crystallogr.* **26**.
Macedo-Ribeiro, S., Darimont, B., Sterner, R. & Huber, R. (1996). *Structure*, **4**, 1291–1301.
Sham, S., Calzolai, L., Wang, P., Bren, K. L., Haarklau, H., Brereton, P. S., Adams, M. W. W. & La Mar, G. N. (2002). *Biochemistry*, **41**, 12498–112508.
Vagin, A. & Teplyakov, A. (1997). *J. Appl. Cryst.* **30**, 1022–1025.
Wang, P., Calzolai, L., Bren, K. L., Teng, Q., Jenney, F. E., Brereton, P. S., Howard, J. B., Adams, M. W. W. & La Mar, G. N. (1999). *Biochemistry*, **38**, 8167–8178.
Zhang, J., Christensen, H. E. M., Ooi, B. L. & Ulstrup, J. (2003). Submitted.